

COMPLEX NUMERICAL AND EXPERIMENTAL RESEARCH OF HEXAFLY-INT HIGH-SPEED CIVIL AIRCRAFT MODEL

V.Yu. Aleksandrov*, S.N. Batura*, O.V. Gouskov*, N.V. Kukshinov*, A.N. Prokhorov*,
A.V. Rudinsky*

*Central Institute of Aviation Motors named after P.I. Baranov (CIAM), Russian
Federation

Keywords: *scramjet, HEXAFLY-INT, CFD, ground tests*

Abstract

The paper presents the results of computational and experimental studies of the characteristics of the high-speed experimental flight test vehicle EFTV with a power plant conducted within the framework of the HEXAFLY-INT project. The results of a numerical study of the combustion of hydrogen in the combustion chamber of EFTV are presented. For the main trajectory points, numerical studies were carried out to evaluate the efficiency of the working process in the chamber and to study the structure of the flow by varying the parameters of the oncoming flow and fuel mass-flow rates. The boundaries of the stable operation of the proposed combustion chamber are shown depending on various factors. In the area of experimental studies the results of tests of the facility module on a high-enthalpy facility are given, and the thrust characteristics of facility module are determined.

1 Introduction

In the HEXAFLY project, a scale model of a hypersonic civil aircraft was proposed, the cruise flight of which is carried out at a speed corresponding to the Mach number $M = 7.5$ [1, 2]. The concept of this model formed the basis of the high-speed experimental flight test vehicle EFTV studied within the framework of the HEXAFLY-INT project [3, 4]. The configuration of the EFTV is shown in Fig. 1. In this project, the Central Institute of Aviation Motors (CIAM) participates in the preparation, conduct and analysis of the ground tests of the

facility module, as well as in the numerical modeling of flow around the aircraft and the flow in the flow path of the engine.

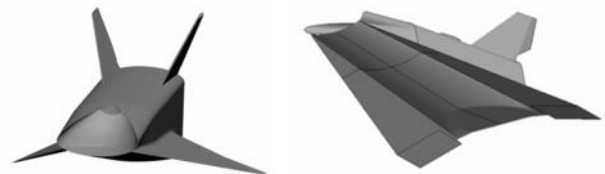


Fig. 1. Configuration of the EFTV HEXAFLY

For testing in CIAM a facility module was designed and manufactured (Fig. 2). It is a scramjet integrated with the intake and installed on a power pylon. There are no external aerodynamic surfaces (wings, elevons and ailerons). Compared with the original modification (Fig. 1), the facility module has a technological intake providing a similar flow structure and the same integral values of the main parameters as the original intake [5, 6].

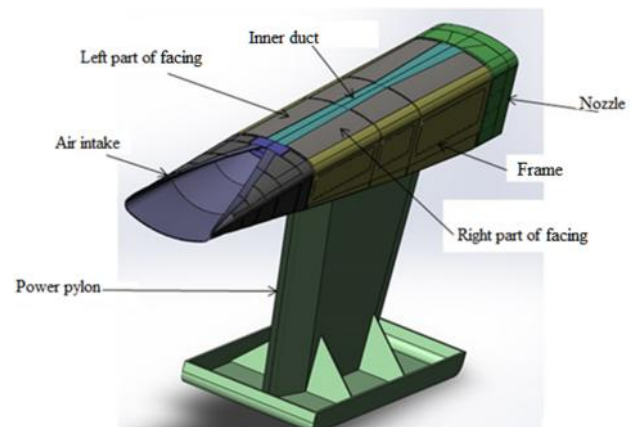


Fig.2.Scramjet facility module of EFTV

2 Numerical simulation of hydrogen combustion

The main design feature of the model is the arrangement of the first belt of the fuel struts near the throat of the air intake, which leads to the need to calculate the flow in the combustion chamber in integration with the air intake of the aircraft. For numerical simulation, the FNAS3D computational program developed at CIAM was used. This program is based on a modified version of the Godunov scheme [7]. Complete Favre averaged system of Navier-Stokes equations for nonstationary turbulent flows of a reacting gas with a closure by means of a one-parameter turbulence model is used [8]. To describe the combustion of a hydrogen-air mixture, the detailed kinetic mechanism of Dimitrov [9] was used.

To estimate the efficiency of processes in the combustion chamber, the combustion efficiency coefficient was used [10, 11]. It should be noted that there are several ways to determine it. In the work, combustion efficiency was defined as the ratio of the amount of heat released in the flow as a result of chemical reactions to the total calorific value of the fuel. The order of calculation was the same for all options. First, the flow around the head part of the apparatus was calculated, to define air mass-flow rate through the throat. After that pressure in the fuel supply system was defined providing the necessary value of the equivalence ration coefficient (ER). At the end, the supply of hydrogen with the given parameters was switched on, and the stationary solution was found.

In the work robustness of the proposed concept in various trajectory points was investigated. The flow parameters at the considered points of the 2 trajectory are presented in Tab. 1. In order to take into account the different paths along the trajectory, calculations at each altitude were performed at different angles of attack. Initially, angles equal to -2° , 0° , 2° and 6° were considered. In addition during the study ER was varied. In this paper we considered three main ER values $ER = 1$; 0,8; 1.2.

Tab. 1. Boundary conditions

H (km)	T (K)	p (Pa)	Mach
35.9	239	502	7,5
27.8	224	165	7

The regime with Mach number of the oncoming flow $M = 7.5$ is characterized by the lowest air and hydrogen mass-flow rates in the combustion chamber. In all the considered variants, a stable supersonic flow was obtained in the combustion chamber with small subsonic zones. We can talk about the stable process in the combustion chamber within the investigated ER and the angles of attack.

Fig. 3 shows the fields of Mach number in the symmetry plane of the combustion chamber at $ER = 1$ and angles of attack $\alpha = -2^\circ$, 0° , 6° . At the considered angles of attack, a similar flow structure is observed with the supersonic flow velocity maintained along the combustion chamber.

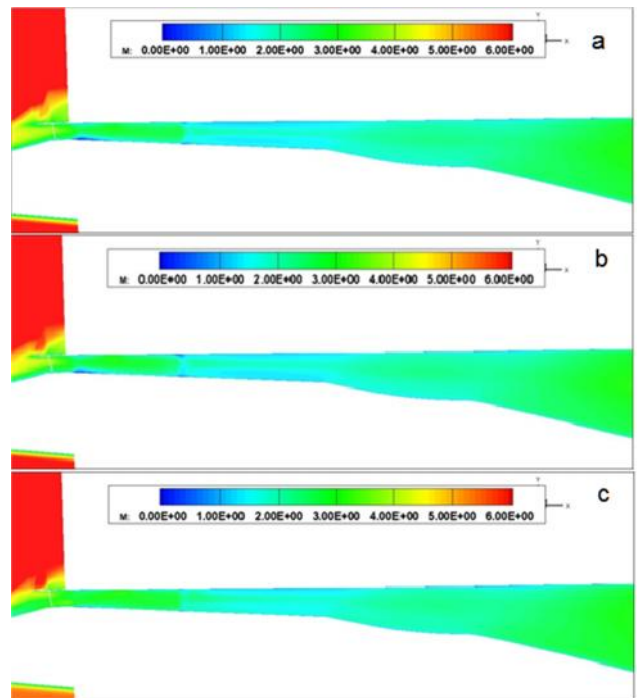


Fig. 3 Mach number fields in symmetry plane of combustion for $M = 7,5$; $ER = 1$; $\alpha = -2^\circ$ (a), $\alpha = 0^\circ$ (b), $\alpha = 6^\circ$ (c)

Fig. 4 shows the fields of mass concentrations of OH radicals for the regime $ER = 1$, $\alpha = 0^\circ$. By zones of formation of OH radicals, one can judge the local character of hydrogen burning and the presence of low-temperature regions in

which combustion does not occur.

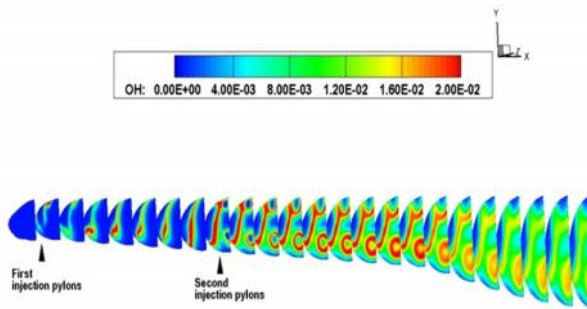


Fig. 4. OH mass concentrations in combustion chamber cross-sections $M=7.5$, $\alpha=0^\circ$, $ER=1$

Despite the similar gas-dynamic character of the flow for variants with different angles of attack, the combustion process can occur with varying rate of efficiency. Fig. 5 shows the distribution combustion efficiency along the length of the chamber for a fixed angle of attack $\alpha = 0^\circ$. The results are presented for three different values of $ER = 0.8$; 1 ; 1.2 . In this case, the combustion efficiency was calculated in relation to the actual fuel mass-flow rate, which was supplied to the flow. Because of this way of determining there is a leap in the chart, it corresponds to the location of the second fuel struts belt. At this point, an additional mass of hydrogen enters the flow, which leads to a decrease in the combustion efficiency then as the mixing and hydrogen enters the reaction, the value of the combustion efficiency increases. According to the presented graph, it is seen that at the same boundary conditions at the inlet, the combustion efficiency increases with the deviation from the stoichiometric ratio.

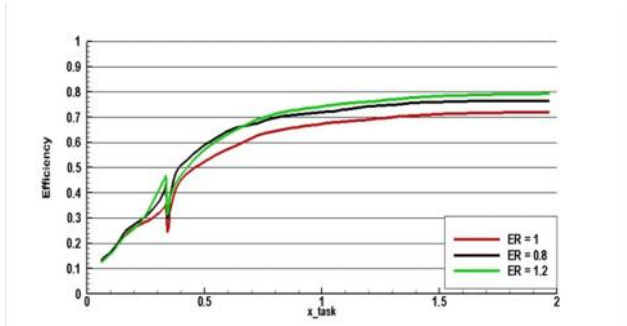


Fig. 5. Combustion efficiency distribution along the flow path for $M=7.5$, $\alpha=0^\circ$

Of the considered trajectory points the $M = 7$ mode is borderline where depending on the angles of attack and ER variants of the stable

supersonic combustion process in the combustion chamber and variants with thermal shocking are observed. At all angles of attack, 3 basic values of the coefficient $ER = 0.8, 1, 1.2$ were calculated. For those angles of attack where the thermal shocking was observed, calculations were performed for other values of the coefficient ER . The ranges where the combustion chamber operates in a normal supersonic mode are determined.

The flow at points with a stable supersonic flow is similar to the fields shown in Fig. 3 - 4. At points with thermal shocking, the flow field with a knocked out shock wave in the air intake device is observed (Fig. 6). The knocked out shock wave leads to a significant reduction of air mass-flow rate.

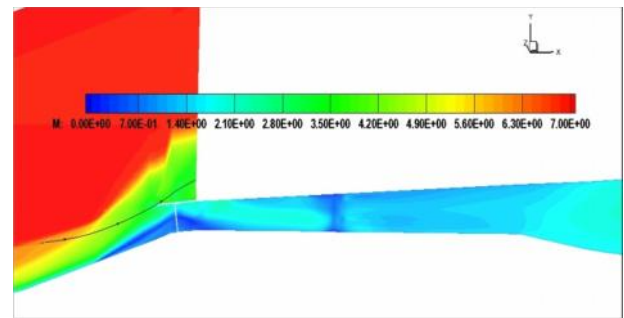


Fig. 6. Mach number field in symmetry plane for $M=7$, $\alpha=-2^\circ$, $ER=1$

As a generalization of the obtained results it could be concluded that for this model the Mach number $M = 7$ is a boundary value in the sense of the stability of combustion process in the combustion chamber. A small change in external parameters, such as the angle of attack, flight altitude, or the ER can lead to a breakdown of the flow in the intake. Fig. 7 shows the range of values at which the combustion chamber operates in normal mode in coordinates the angle of attack - ER . In this graph, the set of values below the curve must provide supersonic flow without thermal shocking.

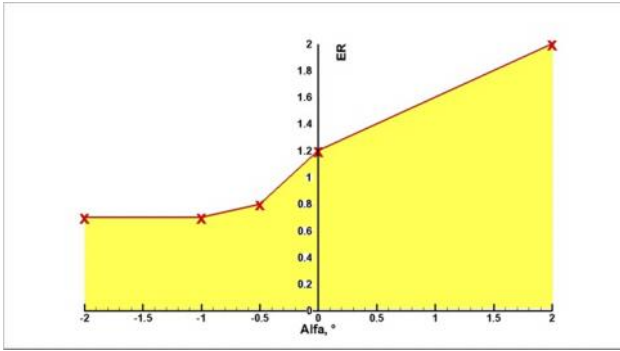


Fig. 7. Combustion chamber normal mode (yellow zone) range for $M=7$ case (ER – Angle of attack coordinates)

3 Experimental research of facility module thrust characteristics

Tests were carried out for positive aero-propulsive balance demonstration and combustion chamber operating process effectiveness evaluation. Tests also allowed to obtain the values of aerodynamic forces affected the facility module. Facility module was mounted on the force-measuring device. Facility module was equipped with pressure sensors for inner duct working process analysis.

In preparation for the tests, computational studies were conducted to determine the regime parameters of the facility under which the flight conditions will be modeled and the intake of the facility module will be started. As a result of the design study, the main test mode was chosen total pressure $p^* = 6.4$ MPa, total temperature $T^* = 2310$ K. The Mach number field in the symmetry plane of the facility for this regime are shown in Fig. 8.

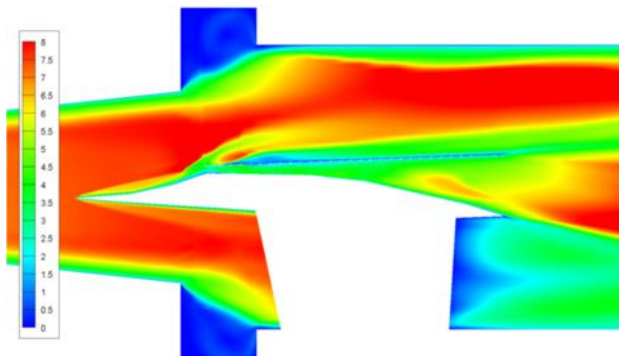


Fig. 8. Mach number field in the symmetry plane $p^* = 6.4$ MPa, $T^* = 2310$ K

During the tests, the equivalence ratio and the percentage of hydrogen flow through the fuel supply belts were varied. A total of 18 runs took place. During the runs the pressure in the vitiation heater was in the range $P_{vh} = 6.1-6.5$ MPa, the temperature $T_{vh} = 2310$ K. The modes and test results are shown in Tab. 2. The modes in which the positive aero-propulsive balance of the facility module was shown are bold. The positive aero-propulsive balance means that thrust generated by the engine, allowed to exceed the total aerodynamic drag.

Tab. 2. Tests results

Point number	P_{vh} , Mpa	ER	Fuel injection through bands, %	Stable working process	Force, N
1	6.177	0.738	1/0	+	-161.8
2	6.283	1.208	0.65/0.35	+	-64.9
3	6.292	1.230	0.61/0.39	+	-43.4
4	6.310	1.291	0.66/0.34	+	-26.8
5	6.353	1.312	0.75/0.25	+	-7.3
6	6.362	1.432	0.77/0.23	-	-360.5
7	6.357	1.431	0.70/0.30	-	-355.7
8	6.397	1.432	0.56/0.44	+	39.3
9	6.419	1.499	0.54/0.46	+	50.1
10	6.431	1.629	0.54/0.46	+	78.9
11	6.428	1.141	0.40/0.60	-	-226.3
12	6.428	1.308	0.43/0.57	-	-136.9
13	6.442	1.525	0.43/0.57	+	63.4
14	6.441	1.751	0.38/0.62	+	85.4
15	6.461	1.183	0.91/0.09	-	-368.7
16	6.452	1.071	1/0	-	-367.4
17	6.474	1.028	0.68/0.32	+	-110.2
18	4.412	1.305	0.70/0.30	-	-109.9

P_{vh} – vitiation heater pressure,

ER – equivalence ratio,

Fuel injection through bands – percentage of fuel going through first/second fuel band,

Stable working process – means stable supersonic combustion in scramjet without thermal choking,

Force – longitudinal force affected on facility module while fuel supplied

It is seen that positive aero-propulsive balance was demonstrated for $ER = 1.43 - 1.75$. Also it was shown that limiting mass-flow rate through the 1st fuel supply band is $G = 18$ g/s. If the mass-flow rate through the 1st band was higher that this value thermal choking was occurred. On figure 9 force time dependence for run 14 is shown. The jump in thrust sensor readings at time $t = 12.5$ s corresponds to the start of the intake. Fuel supply to the combustion chamber was brought into action when vitiation heater pressure was constant therefore it can be assumed that during the work process in combustion chamber the parameters of upcoming flow were not changed. During the

fuel supply to the combustion chamber ($t = 17-18,5$ s) a stable working process providing a positive aero-propulsive balance was demonstrated, the average value of the sum force affecting the object was $R = 85,4$ N. The average value of the aerodynamic drag during testing $X = -360$ N, whereas the calculated value was $X = -394$ N. The difference 9% suggests good accuracy of calculation methods used.

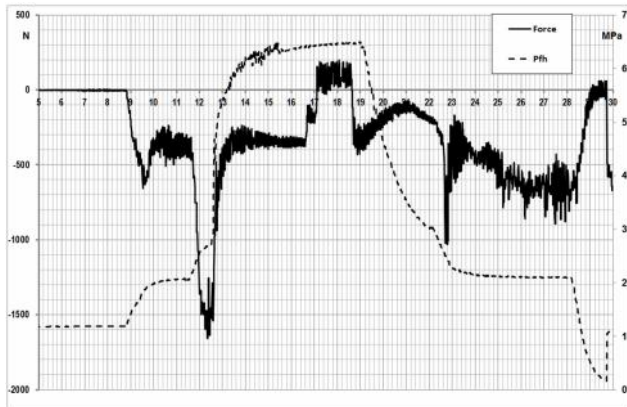


Fig. 9. Longitudinal force (Force, N) and vitiation heater pressure (Pfh, MPa) time dependence

Fig. 10 shows thrust ER dependence. For the thrust of the scramjet there is a tendency to increase with increasing ER with a maximum in the vicinity of $ER = 1.6$. At $ER = 1.629$ the maximum thrust of the scramjet was obtained $T = 308.6$ N. Thrust in experiment was obtained as follows. In the experiments, the longitudinal force acting on the facility module was measured. The flow of the module occurs both before the fuel supply to the combustion chamber and during the supply, while constant values of the parameters of the oncoming flow are maintained. Thus, the force sensor before the fuel supply shows the total aerodynamic drag of the facility module, and during the fuel supply an effective thrust. Assuming that the external drag of the facility module and the flow structure in the air intake do not change in run while the oncoming flow are maintained the thrust can be determined by formula (1).

$$T = \Delta R - I_{\infty} + I_{out_c} \quad (1)$$

where T is the thrust of the engine, ΔR is the experimentally determined difference in the readings of the force sensor when the fuel is supplied and without supply, I is the oncoming

flow impulse, I_{out_c} is the flow impulse at the nozzle exit of the facility module without fuel supply (determined from three-dimensional numerical simulation).

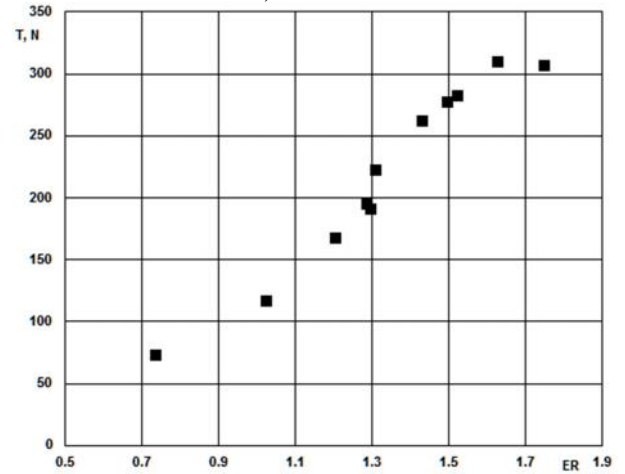


Fig. 10. Thrust ER dependence

Fig. 11 shows the pressure distribution along the length of the flow path in a time moment corresponding to the combustion process in the combustion chamber. Along the length of the inner duct 15 bands of pressure sensors was set, 3 sensors in each band was mounted (on the left side, the right side and center, as shown in the scheme). According distributions a clear peak can be seen in the second part of the combustion chamber between the second fuel struts band and inlet in an expanding part of the nozzle, which shows that in this part of the flow path there is the maximum heat release. Also according to graphs the assumption of a low speed local area presence in the central part of the combustion chamber inlet just behind the intake throat can be made. This area presence is caused by heat release due to 1st struts band fuel combustion. In the runs, where the aero-propulsive balance of the facility module was not demonstrated, but there was a steady burning in the combustor chamber, the pressure distributions and the character of the thrust sensor readings looked similar.

On the distribution of pressure along the flow path validation of calculation methods was carried out. Fig. 12 presents a comparison of calculated and experimental data.

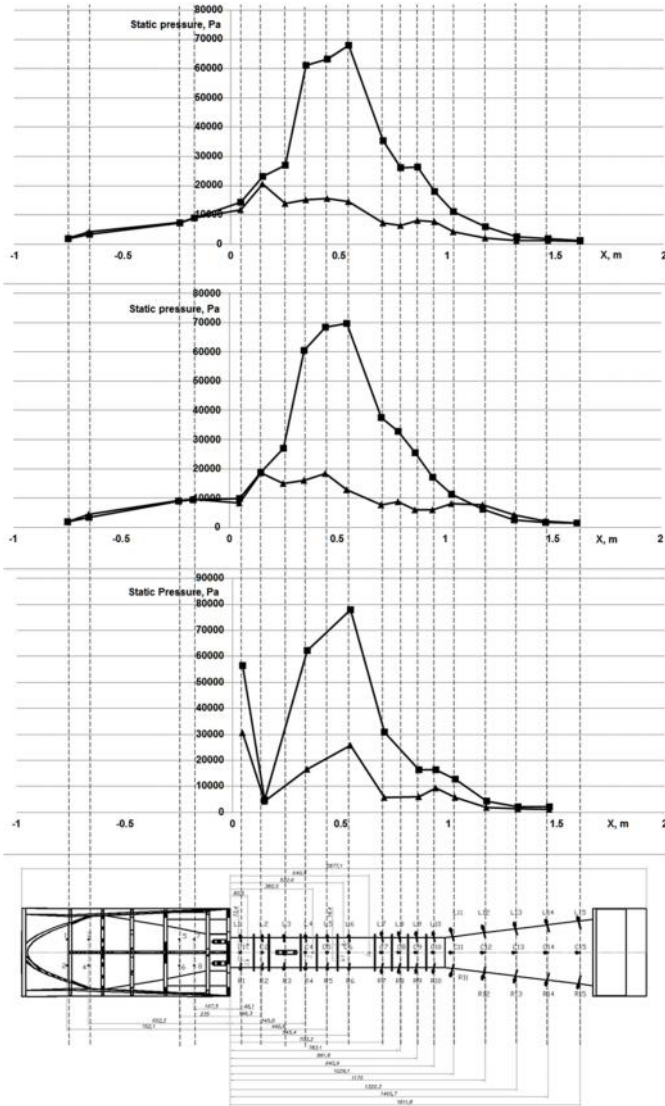


Fig. 11. Pressure distribution along the flow path (top – left sensor band, center – right sensor band, bottom – central sensor band)

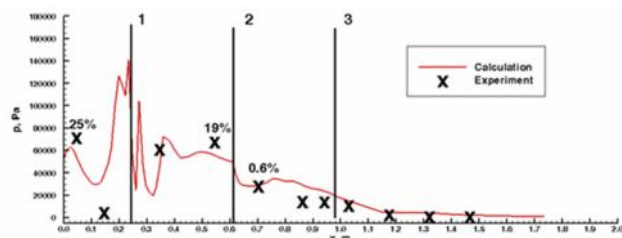


Fig. 12. Numerical and experimental pressure distribution comparison

Fig. 12 shows that at the exit from the combustion chamber the error is 19%. An error of 25% is observed at the entrance to the combustion chamber, and the error level at the second experimental point is more than 100%. This may be due to the unevenness of the oncoming flow in the experiment due to the

peculiarities of the location of the model in the aerodynamic nozzle of the facility. It should be noted that the positions of the maximum and minimum pressure in the places of installation of sensors in the area under consideration are reproduced in calculation. This indicates the qualitative conformity of results. To improve the quantitative agreement of the calculated and experimental data in this area, a more detailed calculation grid should be used. After section 1, good agreement between the calculated and experimental results is observed.

4 Conclusions

The processes of mixing and combustion of the hydrogen-air fuel mixture in the combustion chamber of the HEXAFly-INT model are studied with varying parameters of the oncoming flow and fuel mass-flow rates. The boundaries of the stable operation of the combustion chamber were determined. It is shown that the stable operation of the scramjet with the Mach number of the oncoming flow $M = 7.5$ is realized throughout the considered range of equivalence ratios ($ER = 0.8-1.2$) and angles of attack (from -2 to 6). At Mach number of the oncoming stream $M = 7$ both modes with stable supersonic combustion in combustion chamber and modes with thermal shocking and a knocked out shock wave in the intake were observed.

For the selected regimes $p^* \sim 4.4 - 6.5$ MPa, $T^* \sim 2310$ K, tests were carried out in high-altitude conditions with an oncoming flow velocity corresponding to Mach number $M \sim 7.5$. During the tests the positive aeropropulsive balance of scramjet facility module on hydrogen fuel was demonstrated. The maximum value of the longitudinal force acting on the module $R = 85.4$ N with $ER = 1.75$, the maximum value of the engine thrust $T = 308.6$ N with $ER = 1.63$.

A comparison of the calculated and experimental distribution of pressure along the engine path was made and a satisfactory results agreement was shown.

Acknowledgements

This work was performed within the ‘High Speed Experimental Fly Vehicles - International’ (HEXAFLY-INT) project fostering International Cooperation on Civil High-Speed Air Transport Research. HEXAFLY-INT, coordinated by ESA-ESTEC, is supported by the EU within the 7th Framework Program Theme 7 Transport, Contract no.: ACP3-GA-2014-620327. The project is also supported by the Ministry of Industry and Trade, Russian Federation. Further information on HEXAFLY-INT can be found on http://www.esa.int/techresources/hexafly_int.

References

- [1] Steelant J., Langener T., Hannemann K., Riehmer J., Kuhn M., Dittert C., Jung W., Marini M., Pezzella G., Cicala M., Serre L. Conceptual Design of the High-Speed Propelled Experimental Flight Test Vehicle HEXAFLY. *20th AIAA International Space Planes and Hypersonic Systems and Technologies Conference*. Glasgow, Scotland, July 6-9, 2015: AIAA-2015-3539.
- [2] Steelant J., Varvill R., Defoort S., Hannemann K., Marini M. Achievements obtained for sustained hypersonic flight within the LAPCAT-II project. *20th AIAA International Space Planes and Hypersonic Systems and Technologies Conference*. Glasgow, Scotland, July 6-9, 2015: AIAA-2015-3677.
- [3] Steelant J., Marini M., Pezzella G., Reimann B., Chernyshev S.L., Gubanov A.A., Talyzin V.A., Voevodenko N.V., Kukshinov N.V., Prokhorov A.N., Neely A.J., Kenell C., Verstraete D., Buttsworth D. Numerical and Experimental Research on Aerodynamics of High-Speed Passenger Vehicle within the HEXAFLY-INT Project. *30th Congress of the International Council of the Aeronautical Sciences (ICAS)*. Daejeon, Korea, September 26-30, 2016: ICAS-2016-0353.
- [4] Aleksandrov V.Yu., Kukshinov N.V., Prokhorov A.N., Rudinskiy A.V. Analysis of the integral characteristics of HEXAFLY-INT facility module. *21st AIAA International Space Planes and Hypersonic Systems and Technologies Conference*. Xiamen, China, March 6-9, 2017: AIAA-2017-2179.
- [5] Aleksandrov V.Yu., Danilov M.K., Gouskov O.V., Gusev S.V., Kukshinov N.V., Prokhorov A.N., Zakharov V.S. Numerical and experimental investigation of different intake configurations of HEXAFLY-INT facility module. *30th Congress of the International Council of the Aeronautical Sciences (ICAS)*. Daejeon, Korea, September 26-30, 2016: ICAS-2016-0380.
- [6] Karl S., Steelant, J., Cross-Flow Phenomena in Streamline Traced Hypersonic Intakes. *20th AIAA International Space Planes and Hypersonic Systems and Technologies Conference*. Glasgow, Scotland, July 6-9, 2015: AIAA-2015-3594.
- [7] Godunov S.K., Zabrodin A.V., Ivanov M.Ya., Krayko A.N., Prokopov G.P. Numerical calculation of gas dynamic multidimensional problems. Moscow, Nauka, 1976
- [8] Gulyaev A.N., Kozlov V.E., Secundov A.N. To the creating of general one-parameter model for turbulent viscosity. *Fluid mechanics*. 1993, 4, p.69-81.
- [9] Dimitrow V.I. The maximum kinetic mechanism and rate constants in H₂-O₂ system. *React. Kinetic Catal. Lett.* 1977, v.7, N1, p.81-86.
- [10] Arefev K.Yu., Kukshinov N.V., Serpinskiy O.S. Methodology of experimental determining the combustion efficiency of fuel mixture flows in channels of variable cross-section. *Fluid mechanics*. 2017, 5, p.682-694.
- [11] Aver'kov I.S., Aleksandrov V.Y., Aref'ev K.Y., Gus'kov O.V., Prokhorov A.N., Yanovskii L.S., Voronetskiy A.V. The influence of combustion efficiency on the characteristics of ramjets. *High temperature*. 2016, 6, p.882-891.

Contact Author Email Address

The contact author is Nikolay Kukshinov, CIAM, e-mail: kukshinov@ciam.ru

Copyright Statement

The authors confirm that they, and/or their company or organization, hold copyright on all of the original material included in this paper. The authors also confirm that they have obtained permission, from the copyright holder of any third party material included in this paper, to publish it as part of their paper. The authors confirm that they give permission, or have obtained permission from the copyright holder of this paper, for the publication and distribution of this paper as part of the ICAS proceedings or as individual off-prints from the proceedings.